Intra- and Intermolecular Second-Sphere Coordination Chemistry: Formation of Capsules, Half-Capsules, and Extended Structures with Hexaaquo- and Hexaamminemetal Ions

Sean A. Dalrymple, Masood Parvez, and George K. H. Shimizu*

Department of Chemistry, University of Calgary, Calgary, Alberta T2N 1N4, Canada

Received April 2, 2002

In the design of novel extended solids, particularly those based on weaker interactions, reliable "synthons" are a valuable commodity. This work concerns the hydrogen-bonded assemblies which result from the second-sphere coordination interactions between a highly preorganized trisulfonate ligand and hexaaquo metal ions. Significantly, supramolecular structural variation, which may be rationalized on the basis of the features of the molecular building blocks, is observed. The results are formation of second-sphere capsules with trivalent ions (Fe^{3+}, Cr^{3+}, Al^{3+}), and half-capsules with divalent ions (Mg^{2+}, Zn^{2+}). The divalent systems further assemble into extensively hydrogen-bonded hexagonal nets. Effects of geometrical variation of the building blocks are also observed when a Jahn–Teller-distorted divalent ion (Cu^{2+}) is substituted for the perfectly octahedral species. The second-sphere effects on the stabilization of the primary coordination sphere are illustrated by TGA experiments. In these assemblies, the potential of a new supramolecular synthon is illustrated, that being the complementary *cis*-aquo sulfonate interaction. These complexes illustrate the general utility of second-sphere effects, both as an assembly tool and to stabilize metal complexes in the solid state. Finally, as a comparison, a hydrogen-bonded assembly with a hexaammine complex of a trivalent metal (Co^{3+}) is presented, which forms an extended network with a completely altered hydrogen bonding array.

Introduction

Two fundamental points in the design of any architecture, be it macroscopic or molecular, are the physical features of the units to be assembled and the means by which these items are to be held together. The clearer the definition of these criteria, the more certain and meaningful the design process becomes. From a molecular standpoint, trends in covalent bonding, such as for the second-row p-block elements, represent a high degree of certainty. Stronger bonding translates to more regular bonding. As the bond strength scale shifts to weaker noncovalent interactions, there is, in general, a rapid decline in regularity and, hence, relative predictability. One of the primary mandates of supramolecular chemistry is to provide greater insight into these noncovalent interactions and, by exploiting principles of preorganization, multivalency and cooperativity, allow for the generation of new functional assemblies by design.[1] As applied to infinite solids, these are the principles which underpin the discipline of crystal engineering.[2]

There are many reliable "synthons" in supramolecular chemistry. This term refers to molecular couples, typically functional groups or faces of molecules, which have a high degree of complementarity with respect to intermolecular interactions. As such, they are manifested as recurring structural motifs in supramolecular assemblies. For example, there is the complementarity of 2-aminopyridines and carboxylic acids and nitro groups and amines, as well as the self-complementarity of −COOH groups or 2-pyridones. There are a number of excellent reviews dealing with this topic.[3] Molecular units which express these features thus represent predictable building blocks, synthons, for the generation of larger architectures.

Second-sphere coordination,[4] while having been studied fairly extensively for molecular species, has been studied to a much smaller degree in the generation of extended

---

(1) Lehn, J.-M. *Supramolecular Chemistry, Concepts and Perspectives*; VCH: Weinheim, Germany, 1995.

(2) (a) Desiraju, G. R. *Crystal Engineering: The Design of Organic Solids*; Elsevier: New York, 1989. (b) Desiraju, G. R. *Chem. Commun.* **1997**, 1475.

architectures. While more and more coordination frameworks are being generated where two distinct functionalities appear in the same ligand, one to coordinate the metal and one typically to form hydrogen bonds,[5] it is uncommon that a ligand as simple as water is employed as a supramolecular synthon.[6] Second-sphere coordination refers, in general, to any interactions with the primary coordination sphere of a ligated metal ion.[4] These phenomena have a fundamental role in the physical behavior of a metal complex, and past studies have focused on charge transfer,[7] transport,[8] stability,[9] and even nuclear relaxivity.[10] Given the inherent inter-molecular nature of these interactions, their implementation as a means of assembling metal complexes is a logical extension of the chemistry of discrete species. This work is concerned with a trisulfonated mesitylene ligand, **L**, and its
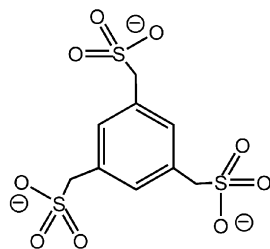
second-sphere hydrogen-bonded assemblies with hexaaquo- and hexaamminemetal complexes. The ligand has a virtually perfect conformation to cap the triangular face of a hexaaquo octahedral metal complex. These *intra*molecular[11] second-sphere interactions form capsules and half-capsules with

trivalent and divalent hexaaquometal complexes, respectively. For the divalent systems, further *inter*molecular[11] second-sphere interactions result in the assembly of discrete units into frameworks with hexagonal channel systems. In these aquo structures, the predominant hydrogen-bonding motif is the complementarity between *cis*-aquo ligands on the metal centers and two adjacent oxygen atoms of a sulfonate group. This interaction has not been previously recognized as a use-ful supramolecular synthon, although it has been observed.[12] In contrast, with a hexaammine primary coordination sphere, the predominant hydrogen bonding tendency is for individual sulfonate oxygen atoms to bridge or cap *cis*-NH_3 sites on the metal which subsequently promotes intermolecular[11] aggregation and the formation of extended structures. We present, herein, the following complexes of **L**:[13] trivalent hexaaquometal ions which form fully encapsulated species,[13] $\{Fe(H_2O)_6\}[Fe(H_2O)_6(\mathbf{L})_2]\cdot6MeOH$, **1**, $\{Cr(H_2O)_6\}[Cr(H_2O)_6(\mathbf{L})_2]\cdot6MeOH$, **2**, $\{Al(H_2O)_6\}[Al(H_2O)_6(\mathbf{L})_2]\cdot6MeOH$, **3**; half-encapsulated complexes with divalent hexaaquo ions, $[Zn_{1.5}(H_2O)_9\mathbf{L}]$, **4**, $[Mg_{1.5}(H_2O)_9\mathbf{L}]$, **5**; the related Jahn−Teller distorted complex, $[Cu_{1.5}(H_2O)_9\mathbf{L}]\cdot1.3H_2O$, **6**; the extended network, $[Co(NH_3)_6(\mathbf{L})]$, **7**, which results with a trivalent hexaammine complex. Each of these structures can be fully justified on the basis of differences in charge, geometry, and ligation of the parent metal complexes and, importantly, the degree of complementarity between the primary coordination sphere on the metal and the second coordination sphere provided by the trisulfonated mesitylene ligand.

Experimental Section

Materials and Methods. Commercial reagents and solvents were purchased from Aldrich and used without further purification. 1,3,5-Tris(bromomethyl)benzene was prepared by a literature procedure.[14]

(3) (a) Moulton, B.; Zaworotko, M. J. *Chem. Rev.* **2001**, *101*, 1629. (b) Nangia, A.; Desiraju, G. R. *Top. Curr. Chem.* **1998**, *198*, 57. (c) Aakeroy, C. B.; Seddon, K. R. *Chem. Soc. Rev.* **1993**, *22*, 397. (d) Blake, A. J.; Champness, N. R.; Hubberstey, P.; Li, W. S.; Withersby, M. A.; Schröder, M. *Coord. Chem. Rev.* **1999**, *183*, 117. (e) Zhang, H.; Wang, X. M.; Zhang, K. C.; Teo, B. K. *Coord. Chem. Rev.* **1999**, *183*, 157. (f) Braga, D.; Grapioni, F.; Desiraju, G. R. *Chem. Rev.* **1998**, *98*, 1375. (g) Aakeroy, C. B.; Beatty. A. M. *Aust. J. Chem.* **2001**, *54*, 409.
(4) (a) Loeb, S. J. In *Comprehensive Supramolecular Chemistry*; Atwood, J. L., Davies, J. E. D., MacNicol, D. D., Vögtle, F., Eds.; Elsevier Science: New York, 1996; Vol. 1, p 733. (b) Raymo, F. M.; Stoddart, J. F. *Chem. Ber.* **1996**, *129*, 981. (c) Zamaraev, K. *New J. Chem.* **1994**, *18, 3*.
(5) (a) Burrows, A. D.; Chan, C. W.; Chowdhry, M. M.; McGrady, J. E.; Mingos, D. M. P. *Chem. Soc. Rev.* **1995**, *24*, 329. (b) Beatty, A. *Cryst. Eng. Commun.* **2001**, *51*, 1. (c) Aakeroy, C. B.; Borovik, A. S. *Coord. Chem. Rev.* **1999**, *183*, 1. (d) Braga, D.; Maini, L.; Polito, M.; Scaccianoce, L.; Cojazzi, C.; Grepioni, F. *Coord. Chem. Rev.* **2001**, *216*, 225.
(6) (a) Cusack, P. A.; Bhagwati, N. P.; Smith, P. J. *J. Chem. Soc., Dalton Trans.* **1984**, 1239. (b) Valle, G.; Cassol, A., Russo, U. *Inorg. Chim. Acta* **1984**, *82*, 81. (c) Dalrymple, S. A.; Shimizu, G. K. H. *Chem. Commun.* **2002**, 2224. (d) Beauchamp, D. A.; Loeb, S. J. *Chem. Eur. J.* **2002**, *8*, 5084.
(7) Zhou, P.; Au-Yeung, S. C. F.; Xu, X.-P. *J. Am. Chem. Soc.* **1999**, *121*, 1030.
(8) Crumbliss, A. L.; Batinić -Haberle, I.; Spasojević, I. *Pure Appl. Chem.* **1996**, *68*, 1225.
(9) Siegbahn, P. E. M.; Crabtree, R. H. *Mol. Phys.* **1996**, *89*, 279.
(10) (a) Botta, M. *Eur. J. Inorg. Chem.* **2000**, 399. (b) Bleuzen, A.; Foglia, F.; Furet, E.; Helm, L.; Merbach, A.; Weber, J. *J. Am. Chem. Soc.* **1996**, *118*, 777. (c) Bertini, I.; Fragai, M.; Luchinat, C.; Parigi, G. *Inorg. Chem.* **2001**, *40*, 4030.
(11) As mentioned, second-sphere interactions are inherently intermolecular. The use of intra- and intermolecular in the context given refers, in essence, to intra- and intersupramolecular interactions as the completely encapsulated $[M(H_2O)_6(\mathbf{L})_2]^{3-}$ and the half-encapsulated $[M(H_2O)_6(\mathbf{L})]^{-}$ species are treated as molecular species to facilitate discussion of their extended organization.

(12) A search of the Cambridge Structural Database for metal complexes with *cis*-aquo ligands and sulfonate anions, employing the Mercury program to elucidate hydrogen bonding, gave 226 hits. Of these 226 compounds, over half (127 or 56.2%) showed the hydrogen-bonding motif, depicted in the Introduction, between the aquo ligands and two adjacent sulfonate oxygen atoms. The next most common motif involves hydrogen bonds to a single sulfonate oxygen atom. It should be noted that these statistics represent the occurrence of this interaction when they have not been specifically targeted as a supramolecular synthon. For representative examples of *cis*-aquo doubly hydrogen bonding, see: (a) Hagen, K. S. *Inorg. Chem.* **2000**, *39*, 5867. (b) Walsh, B.; Hathaway, B. J. *J. Chem. Soc., Dalton Trans.* **1980**, 681. (c) Atwood, J. L.; Orr, G. W. Means, N. C.; Hamada, F.; Zhang, H.; Bott, S. G.; Robinson, K. D. *Inorg. Chem.* **1992**, *31*, 603. (d) Takahashi, Y.; Akita, M.; Kichi, S. H.; Moro-oka, Y. *Inorg. Chem.* **1998**, *37*, 3186. (e) Hernandez-Molina, R.; Dybtsev, D. N.; Fedin, U. P.; Elsegood, M. R. J.; Clegg, W.; Sykes, A. G. *Inorg. Chem.* **1998**, *37*, 2995. (f) Tandon, S. S.; Mandel, S. K.; Thompson, L. K.; Hynes, R. K. *Inorg. Chem.* **1992**, *31*, 2215. (g) Airey, S.; Drljaca, A.; Hardie, M. J.; Raston, C. L. *Chem. Commun.* **1999**, 1137. (h) Johnson, C. P.; Atwood, J. L.; Steed, J. W.; Bauer, C. B.; Rogers, R. D. *Inorg. Chem.* **1996**, *35*, 2602. (i) Funaioli, T.; Cavezza, C.; Marchetti, F.; Fachinetti, G. *Inorg. Chem.* **1999**, *38*, 3361. (j) Gunderman, B. J.; Kabell, I. D.; Squattrito, P. J.; Dubey, S. N. *Inorg. Chim. Acta* **1997**, *258*, 237. (k) Turokowski, P. N.; Bino, A.; Lippard, S. J. *Angew. Chem., Int. Ed. Engl.* **1990**, *29*, 811. (l) Sakane, G.; Hachimoto, K.; Takahashi, M.; Takeda, M.; Shibahara, T. *Inorg. Chem.* **1998**, *37*, 4231. (m) Holt, D. G. L.; Larkworthy, C. F.; Povey, D. C.; Smith, G. W.; Leigh, G. J. *Inorg. Chim. Acta* **1990**, *169*, 201. (n) Ruiz, J.; Florenciano, F.; Vicente, C.; Ramirez de Arellano, M. C.; Lopez, G. *Inorg. Chem. Commun.* **2000**, *3*, 73.
(13) Complexes **1**−**3** have been the subject of a preliminary communica-tion: Dalrymple, S. A.; Parvez, M.; Shimizu, G. K. H. *Chem. Commun.* **2001**, 2672.

^{1}H and ^{13}C NMR spectra were obtained using a Bruker AC-200 nuclear magnetic resonance spectrometer equipped with a Tecmag PowerMac Data system. Electrospray-ionization mass spectra (ESI-MS) were obtained on a Bruker Esquire 3000 spectrometer. Fourier transform infrared (FT-IR) spectra were obtained as KBr pellets on a Nicolet Nexus 470 instrument. Elemental analyses (C, H) were conducted by the Department of Analytical Services at the University of Calgary. Thermogravimetric analysis (TGA) and differential scanning calorimetry were performed on a Netzsch 449C simultaneous thermal analyzer under a static N_2 atmosphere at a scan rate of 5 °C/min.

Synthesis of 1,3,5-Tris(sulfomethyl)benzene, Sodium Salt Hydrate (Na$_3$L). 1,3,5-Tris(bromomethyl)benzene (1.700 g, 4.763 mmol) was added to a solution of Na_2SO_3 (1.801 g, 14.29 mmol) in H_2O (40 mL) and refluxed for 20 h. Removal of the solvent afforded a white powder which was purified by redissolving in H_2O (20 mL) followed by MeOH precipitation (40 mL). After sitting for 10 h at 4 °C, the white crystalline solid was isolated by suction filtration: yield, 1.724 g (4.043 mmol, 85%); mp; ^{1}H NMR (200 MHz, CDCl$_3$) δ (ppm) = 7.28 (s, 3H, arom), 4.07 (s, 6H, CH$_2$SO$_3$); ^{13}C{^{1}H} δ (ppm) = 132.52, 132.02 (arom), 56.79 (CH$_2$SO$_3$); ESI-MS m/z 402.9 [M − Na]$^-$, 380.8 [M − 2Na + H]$^-$, 358.8 [M − 3Na + 2H]$^-$. Anal. Calcd for [(C$_9$H$_9$S$_3$O$_9$)(Na$_3$)]·H$_2$O: C, 24.33; H, 2.50. Found: C, 24.35; H, 2.46. Conversion of the ligand to the acid form (H$_3$L) was accomplished by passing an aqueous solution of Na$_3$L (1.004 g, 2.355 mmol) down an ion exchange column (Dowex 50x8) previously charged with 6 M HCl: yield based on H$_3$L·3H$_2$O, 0.801 g (1.933 mmol, 93%); ^{1}H NMR (200 MHz, D$_2$O) δ = 7.31 (s, 3H, arom), 4.10 (s, 6H, CH$_2$SO$_3$); ^{13}C{^{1}H} δ = 132.44, 131.95 (arom), 56.73 (CH$_2$SO$_3$); ESI-MS m/z 358.9 [M − H]$^-$, 295.0 [M − SO$_2$H]$^-$, 278.9 [M − SO$_3$H]$^-$; mp 210 °C. Anal. Calcd for [H$_3$(L)]·3H$_2$O: C, 26.08; H, 4.38. Found: C, 26.02; H, 4.70.

Syntheses of Compounds 1−3, [(M(H$_2$O)$_6$)[M(H$_2$O)$_6$(L)$_2$]·6MeOH (M = Fe^{3+}, 1, Cr^{3+}, 2, and Al^{3+}, 3). A solution of the ligand was prepared by dissolving Na$_3$L (0.210 g, 0.494 mmol) in H$_2$O (5 mL). To this solution was added an equimolar amount of the appropriate metal salt (Fe(NO$_3$)$_2$·6H$_2$O for **1**, CrCl$_3$·6H$_2$O for **2**, AlCl$_3$·6H$_2$O for **3**). After 10 h, the solutions were translucent in appearance. Diffusion of methanol into these solutions gave single crystals of the desired products after 10 days. Data for **1**: yield, 75%; IR (cm^{-1}, KBr) 3459.2 (br), 1651.0 (s), 1634.6 (s), 1459.8 (m), 1421.6 (m), 1285.0 (s), 1186.6 (vs), 1121.1 (vs), 1050.1 (vs), 766.0 (s), 733.2 (m), 667.7 (s), 585.7 (m), 514.7 (m); DSC/TGA 70−120 °C (417.7 J/g endo) −15.88% obsd and −15.56% calcd for loss of 6 CH$_3$OH, 120−180 °C (70.4 J/g endo) −8.95% obsd and −8.75% calcd for loss of 6 H$_2$O, 180−270 °C (53.0 J/g endo) −8.99% obsd and −8.75% calcd for loss of 6 H$_2$O, 340 °C decomposition of **L**. Anal. Calcd: C, 23.34; H, 5.39. Found: C, 22.93; H, 5.36. Data for **2**: yield, 77%; IR (cm^{-1}, KBr) 3497.4 (br), 1651.0 (s), 1634.6 (s), 1454.3 (s), 1274.0 (s), 1208.5 (vs), 1186.6 (vs), 1121.1 (vs), 1050.1 (vs), 776.9 (s), 667.7 (s), 514.7 (s); DSC/TGA 70−195 °C (696.4 J/g endo) −24.63% obsd and −24.47% calcd for loss of 6 H$_2$O and 6 CH$_3$OH, 195−295 °C (8.22 J/g endo) −8.98% obsd and −8.81% calcd for loss of 6 H$_2$O, 295 °C decomposition of **L**. Anal. Calcd: C, 23.49; H, 5.42. Found: C, 22.87; H, 5.36. Data for **3**: yield, 71%; IR (cm^{-1}, KBr) 3448.2 (br), 1651.0 (s), 1634.6 (s), 1459.8 (m), 1274.0 (s), 1219.4 (s), 1175.7 (s), 1126.6 (s), 1061.0 (vs), 1022.8 (s), 782.4 (s), 769.1 (m), 656.8 (s), 520.2 (vs); DSC/TGA 25−105 °C (501.1 J/g endo for first two mass losses combined) −25.54% obsd and −25.51% calcd for loss of 6 CH$_3$OH and 6 H$_2$O, 180−260 °C (60.55 J/g

endo) −9.31% obsd and −9.18% calcd for loss of 6 H$_2$O, 290 °C decomposition of **L**. Anal. Calcd: C, 17.50; H, 4.41. Found: C, 17.26; H, 3.86.

Synthesis of Compound 4, [Zn$_{1.5}$(H$_2$O)$_9$L]. Na$_3$L (0.194 g, 0.454 mmol) was dissolved in H$_2$O (10 mL) to give a clear colorless solution. Addition of white crystalline Zn(NO$_3$)$_2$·6H$_2$O (0.203 g 0.681 mmol) to the ligand solution resulted in the immediate dissolution of the metal salt without any visible change to the appearance of the solution. After 24 h of stirring, the solution was filtered and ethanol was diffused in. Colorless prismatic crystals were observed after 28 days of solvent diffusion: yield, 0.131 g (0.215 mmol, 32%); IR (cm^{-1}, KBr) 3563.0 (br), 2983.9 (w), 2929.3 (w), 1634.6 (s), 1612.8 (s), 1465.3 (m), 1416.1 (w), 1268.6 (s), 1219.4 (s), 1192.1 (s), 1137.5 (s) 1044.6 (vs), 891.6 (m), 776.0 (s), 667.7 (m), 580.3 (s), 525.64 (s); DSC/TGA 40−160 °C (669.6 J/g endo for first two mass losses combined) −22.00% obsd and 23.34% calcd for loss of 8 H$_2$O, 160−300 °C −2.01% obsd and −2.91% calcd for loss of 1 H$_2$O, 350 °C decomposition of **L**. Anal. Calcd for **4**: C, 17.50; H, 4.41. Found: C, 17.26; H, 3.86.

Synthesis of Compound 5, [Mg$_{1.5}$(H$_2$O)$_9$L], and Compound 6, [Cu$_{1.5}$(H$_2$O)$_9$L]·1.3H$_2$O. To a clear colorless solution of H$_3$L (ca. 0.4 mmol) in H$_2$O (8 mL) was added crystalline M(OH)$_2$ (**5**, M = Mg^{2+}; **6**, M = Cu^{2+}) (ca. 0.6 mmol) which did not immediately dissolve. After 10 min of stirring, the M(OH)$_2$ had almost completely dissolved to give a translucent solution. For **5**, slow diffusion of ethanol into the aqueous solution resulted in colorless prismatic crystals being formed after 6 days of recrystallization. The crystals were isolated by suction filtration for 1 h before being weighed: yield, 55%; IR (cm^{-1}, KBr) 3328.1 (br), 3000.3 (m), 2945.7 (m), 1667.4 (vs), 1629.1 (vs), 1459.8 (s), 1421.6 (s), 1268.6 (s), 1186.6 (s), 1132.0 (s), 1039.1 (vs) 1000.9 (s), 897.1 (s), 782.4 (s), 673.1 (m), 569.4 (m), 514.7 (m); DSC/TGA 70−180 °C (920.1 J/g endo for first two mass losses combined) −27.03% obsd and 25.92% calcd for loss of 8 H$_2$O, 180−260 °C −2.02% obsd and −3.24% calcd for loss of 1 H$_2$O, 400 °C decomposition of **L**. Anal. Calcd for **5**: C, 19.44; H, 4.90. Found: C, 20.69; H, 5.17. For **6**, blue prismatic crystals formed after 5 days of acetone diffusion: yield, 40%; IR (cm^{-1}, KBr) 3492.0 (br), 2962.1 (w), 2923.8 (w), 1634.6 (s), 1618.2 (s), 1459.8 (w), 1427.0 (w), 1268.6 (m), 1219.4 (s), 1197.6 (vs), 1137.5 (s) 1044.6 (vs), 891.6 (m), 776.93 (s), 662.2 (m), 585.7 (s), 585.7 (s), 531.1 (s); DSC/TGA 30−240 °C (477.0 J/g endo) −28.28% obsd and 29.10% calcd for loss of 10.3 H$_2$O, 260 °C decomposition of **L**. Anal. Calcd for **6**: C, 16.94; H, 4.67. Found: C, 17.46; H, 4.55. For **5** and **6**, if the same reaction conditions are employed but with Na$_3$L and MgCl$_2$·2H$_2$O or CuCl$_2$·2H$_2$O, respectively, as the starting materials, only pure Na$_3$L was obtained from the recrystallizations.

Synthesis of Compound 7, [Co(NH$_3$)$_6$]$_2$(L$_1$)$_2$·6H$_2$O. A clear colorless solution of the ligand was prepared by dissolving Na$_3$L (0.254 g, 0.595 mmol) in H$_2$O (10 mL). To this solution was added orange [Co(NH$_3$)$_6$]Cl$_3$ (0.160 g, 0.595 mmol) which initially gave a clear orange solution upon stirring. After approximately 5 min, an orange solid precipitated from solution. Single crystals were grown by dissolving the orange solid in a minimum amount of boiling water and allowing the solution to cool to room temperature after filtration: yield, 0.278 g (0.444 mmol, 74%); IR (cm^{-1}, KBr) 3497.4 (br), 3410.0 (br), 3289.8 (br), 1651.0 (m), 1629.1 (m), 1461.3 (w), 1423.5 (w), 1345.07 (s), 1257.7 (w), 1197.6 (vs), 1121.1 (s), 1044.6 (vs), 875.3.0 (m), 760.6 (m), 667.7 (m), 558.4 (s), 548.4 (m). Anal. Calcd for **7**: C, 18.88; H, 5.81; N, 14.68. Found: C, 18.89; H, 5.67; N, 14.58.

General X-ray Crystallography. Data for **1−3** were collected on a Rigaku AFC6S diffractometer and solved using the teXsan

(14) Vögtle, F.; Zuber, M.; Lichenthaler, R. G. *Chem. Ber.* **1973**, *106*, 717.

Table 1. Crystal Data and Refinement Summary for Compounds **1**–**7**

	1	**2**	**3**	**4**	**5**	**6**	**7**
formula	$C_{12}H_{33}FeO_{18}S_3$	$C_{12}H_{33}CrO_{18}S_3$	$C_{12}H_{33}AlO_{18}S_3$	$C_9H_{27}Mg_{1.5}O_{18}S_3$	$C_9H_{27}Zn_{1.5}O_{18}S_3$	$C_9H_{27}Cu_{1.5}O_{19.25}S_3$	$C_9H_{27}CoN_6O_{12}S_3$
fw	617.41	613.56	588.54	555.95	617.54	634.80	566.48
cryst system	trigonal	trigonal	trigonal	hexagonal	hexagonal	monoclinic	triclinic
space group	$R\bar{3}h$	$R\bar{3}h$	$R\bar{3}h$	$P6_3$	$P6_3$	$P2_1/n$	$P\bar{1}$
a (Å)	13.979(2)	13.936(1)	13.904(2)	12.085(2)	12.0673(6)	11.944(2)	7.903(2)
b (Å)	13.979(2)	13.936(1)	13.904(2)	12.085(2)	12.0673(6)	9.418(2)	14.484(3)
c (Å)	23.869(3)	23.701(3)	23.799(4)	9.662(2)	9.7020(4)	21.553(4)	20.606(4)
α (deg)	90	90	90	90	90	90	89.18(3)
β (deg)	90	90	90	90	90	94.45(3)	89.45(3)
γ (deg)	120	120	120	120	120	90	77.56(3)
V (Å^3)	4039.4(8)	3986.2(7)	3984.7(8)	1222.0(3)	1223.5(1)	2417.1(8)	2303.0(8)
T (°C)	−100	−100	−100	−100	−100	−100	−100
Z	12	12	12	2	2	4	2
D_{calc} (g/cm^3)	1.523	1.534	1.472	1.511	1.676	1.744	1.634
μ (mm^{-1})	0.866	0.740	0.387	0.417	1.813	1.673	1.083
λ (Å)	0.709 30	0.709 30	0.709 30	0.709 30	0.709 30	0.709 30	0.709 30
R_F (sig reflcns)^a	0.0276	0.0286	0.0323	0.0519	0.0601	0.0434	0.0878
R_w (sig reflcns)^a	0.0726	0.0806	0.0857	0.1359	0.1487	0.1045	0.2094

^{a} $R_F = (\sum(F_o - F_c)/\sum(F_o))$; $R_w = (\sum w(F_o - F_c)^2/\sum w(F_o)^2)^{0.5}$.

software program.[15] Single-crystal X-ray data for **4**–**7** were collected on a Nonius Kappa CCD diffractometer. Empirical absorption corrections were made using the correction routine associated with the Nonius diffractometer. The structures were refined and hydrogen atoms generated as riding spheres to their parent atoms using the SHELXTL '97 suite of programs.[16] Fractional atomic coordinates and bond distances and angles in addition to pertinent crystallographic information for all compounds are available as Supporting Information.

Single-Crystal X-ray Determinations. Compound 1. A yellow blocklike crystal of dimensions $0.30 \times 0.42 \times 0.22$ mm^3 was employed. The lattice parameters are $a = b = 13.979(2)$ Å, $c = 23.869(3)$ Å, $\alpha = \beta = 90°$, $\gamma = 120°$, $V = 4039.4(8)$ Å^3, space group $R\bar{3}$, and $Z = 12$. A total of 1743 reflections were measured, and these were merged to give 1597 unique reflections ($R_{merg} = 0.0195$), 1320 of which were considered to be observed when $I > 4.0\sigma(I)$. A summary of pertinent crystal data is presented in Table 1. Final R values for significant data ($R = 2.76\%$, $R_w = 7.26\%$, GoF = 1.057) were obtained for a total of 120 parameters. In the last D-map, the deepest hole was -0.344 e/Å^3 and the highest peak 0.275 e/Å^3.

Compound 2. A yellow blocklike crystal of dimensions $0.30 \times 0.30 \times 0.20$ mm^3 was employed. The lattice parameters are $a = b = 13.936(1)$ Å, $c = 23.701(3)$ Å, $\alpha = \beta = 90°$, $\gamma = 120°$, $V = 3986.2(7)$ Å^3, space group $R\bar{3}$, and $Z = 12$. A total of 5131 reflections were measured, and these were merged to give 1809 unique reflections ($R_{merg} = 0.0183$), 1680 of which were considered to be observed when $I > 4.0\sigma(I)$. A summary of pertinent crystal data is presented in Table 1. Final R values for significant data ($R = 2.86\%$, $R_w = 8.06\%$, GoF = 1.077) were obtained for a total of 122 parameters. In the last D-map, the deepest hole was -0.352 e/Å^3 and the highest peak 0.402 e/Å^3.

Compound 3. A colorless blocklike crystal of dimensions $0.35 \times 0.30 \times 0.20$ mm^3 was employed. The lattice parameters are $a = b = 13.904(2)$ Å, $c = 23.799(4)$ Å, $\alpha = \beta = 90°$, $\gamma = 120°$, $V = 3984.7(8)$ Å^3, space group $R\bar{3}$, and $Z = 12$. A total of 1725 reflections were measured, and these were merged to give 1579 unique reflections ($R_{merg} = 0.0227$), 1263 of which were considered to be observed when $I > 4.0\sigma(I)$. A summary of pertinent crystal data is presented in Table 1. Final R values for significant data ($R = 3.23\%$, $R_w = 8.57\%$, GoF = 1.058) were obtained for a

(15) *teXsan Crystal Structure Analysis Program*; Molecular Structure Corp: The Woodlands, TX, 1985, 1992.
(16) *SHELXTL*, version 5.1; Bruker AXS Inc.: Madison, WI, 1997.

total of 122 parameters. In the last D-map, the deepest hole was -0.353 e/Å^3 and the highest peak 0.373 e/Å^3.

Compound 4. A colorless blocklike crystal of dimensions $0.40 \times 0.30 \times 0.30$ mm^3 was employed. The lattice parameters are $a = b = 12.085(2)$ Å, $c = 9.662(2)$ Å, $\alpha = \beta = 90°$, $\gamma = 120°$, $V = 1222.0(3)$ Å^3, space group $P6$ (chiral)$_3$, and $Z = 12$. A total of 9701 reflections were measured, and these were merged to give 1847 unique reflections ($R_{merg} = 0.0471$), 1670 of which were considered to be observed when $I > 4.0\sigma(I)$. A summary of pertinent crystal data is presented in Table 1. Final R values for significant data ($R = 5.19\%$, $R_w = 13.59\%$, GoF = 1.076) were obtained for a total of 110 parameters. In the last D-map, the deepest hole was -0.554 e/Å^3 and the highest peak 0.532 e/Å^3.

Compound 5. A colorless blocklike crystal of dimensions $0.50 \times 0.42 \times 0.20$ mm^3 was employed. The lattice parameters are $a = b = 12.0673(6)$ Å, $c = 9.7020(4)$ Å, $\alpha = \beta = 90°$, $\gamma = 120°$, $V = 1223.5(1)$ Å^3, space group $P6$ (chiral)$_3$, and $Z = 12$. A total of 2615 reflections were measured, and these were merged to give 1557 unique reflections ($R_{merg} = 0.0378$), 1492 of which were considered to be observed when $I > 4.0\sigma(I)$. A summary of pertinent crystal data is presented in Table 1. Final R values for significant data ($R = 6.01\%$, $R_w = 14.87\%$, GoF = 1.091) were obtained for a total of 111 parameters. In the last D-map, the deepest hole was -0.716 e/Å^3 and the highest peak 0.693 e/Å^3.

Compound 6. A blue blocklike crystal of dimensions $0.35 \times 0.30 \times 0.25$ mm^3 was employed. The lattice parameters are $a = 11.944(2)$ Å, $b = 9.418(2)$ Å, $c = 21.553(4)$ Å, $\alpha = 90°$, $\beta = 94.45(3)°$, $\gamma = 90°$, $V = 2417.1(8)$ Å^3, space group $P2_1/n$, and $Z = 4$. A total of 10 116 reflections were measured, and these were merged to give 5484 unique reflections ($R_{merg} = 0.0366$), 3973 of which were considered to be observed when $I > 4.0\sigma(I)$. A summary of pertinent crystal data is presented in Table 1. Final R values for significant data ($R = 4.34\%$, $R_w = 10.45\%$, GoF = 1.030) were obtained for a total of 313 parameters. In the last D-map, the deepest hole was -0.523 e/Å^3 and the highest peak 1.683 e/Å^3.

Compound 7. A blue blocklike crystal of dimensions $0.50 \times 0.35 \times 0.30$ mm^3 was employed. The lattice parameters are $a = 7.903(2)$ Å, $b = 14.484(3)$ Å, $c = 20.606(4)$ Å, $\alpha = 89.18(3)°$, $\beta = 89.45(3)°$, $\gamma = 77.56(3)°$, $V = 2303.0(8)$ Å^3, space group $P\bar{1}$, and $Z = 2$. A total of 19 292 reflections were measured, and these were merged to give 10 369 unique reflections ($R_{merg} = 0.0485$), 7441 of which were considered to be observed when $I > 4.0\sigma(I)$. A summary of pertinent crystal data is presented in Table 1. Final R values for significant data ($R = 8.78\%$, $R_w = 20.94\%$, GoF =

1.097) were obtained for a total of 571 parameters. In the last *D*-map, the deepest hole was −1.129 e/Å³ and the highest peak 2.623 e/Å³.

Results and Discussion

Structures of Fully Encapsulated Species: $\{M(H_2O)_6\}$-$[M(H_2O)_6(L)_2]\cdot6MeOH$ (M = Fe^{3+}, **1**, Cr^{3+}, **2**, and Al^{3+}, **3).** With the factoring of both electrostatic effects and the high complementarity of the trisulfonate **L** with the triaquo faces of octahedral $[M(H_2O)_6]^{3+}$ cations, second-sphere capsules are formed.[17] The single-crystal X-ray structure determinations of the trivalent hexaaquo metal complexes, **1–3**, reveal these compounds are highly symmetrical and isostructural. The asymmetric units consist of one-third of a molecule of **L**, one methanol molecule, one-sixth of each of the two crystallographically unique metal centers, and two water molecules, one coordinated to each metal ion. A detailed description of only the Fe complex, **1**, will be presented as the Cr and Al complexes are identical to **1** except for very slight variations in structural and thermal parameters which may be ascertained from the Supporting Information. Interestingly, Al^{3+} and Cr^{3+} frequently form isomorphous structures in extended solids (e.g. in ordinary alums, $KM(SO_4)_2\cdot12H_2O$). This is a textbook case of similarities in charge and radius (Al^{3+} = 0.675 Å, Cr^{3+} = 0.755 Å) taking precedent over electronic configuration.[18]

The crystal structure of **1** shows two types of hexaaquo Fe^{3+} centers in the complex. The first center, Fe1, is completely encapsulated by two molecules of **L** through a total of 12 hydrogen bonds, 6 to each molecule of **L** (Figure 1) which forms an overall trianionic complex. The methylsulfonate groups on each molecule of **L** adopt a cis–cis–cis orientation (i.e. they are all on the same side of the benzene core) and cap one of the triangular faces of the octahedral hexaaquo Fe1 center. All six water molecules of Fe1 are crystallographically equivalent (Fe1–O1 = 1.996(2) Å). Both H atoms of the coordinated water molecule form hydrogen bonds to two sulfonate oxygen atoms from two different sulfonate groups (O1···O4 = 2.632(2) Å, O1···O5 = 2.639(2) Å). Thus, each triangular triaquo face of the Fe
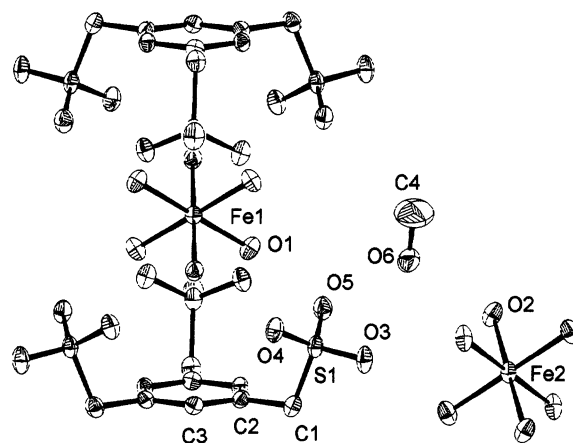

Figure 1. ORTEP plot of **1** showing the numbering scheme and the complete encapsulation of the hexaaquo Fe1 center and the "naked" Fe2 complex. Thermal ellipsoids of 50% probability are represented.

complex is staggered with respect to the 1,3,5-substitution pattern of **L** (Figure 9a). As will be observed to be a regular feature in these aquo complexes, each SO_3 group forms two hydrogen bonds to two water molecules occupying cis coordination sites on the metal. Interestingly, if one envisions RNH_2 in place of $M(H_2O)$, the hydrogen-bonding motif observed for each triaquo face is identical to that in the quasi-hexagonal layers observed by Ward et al. in their guanidinium sulfonate structures.[19]

The hexaaquo Fe2 center is not encapsulated by **L** but rather is interspersed between the trianionic second-sphere complexes in an efficient charge-compensating manner. It also contains only a single crystallographic type of water molecule (Fe2–O2 = 1.986(2) Å). Although Fe2 is not encapsulated, it still participates in significant hydrogen-bonding interactions. There are H-bonds between the coordinated water molecules on Fe2 and O3, the sulfonate oxygen atom not involved in H-bonding to the water molecules of Fe1 (O2···O3 = 2.644(3) Å) as well as to the methanol solvate molecules (O6···O2 = 2.563(3) Å). Therefore, in total, each hexaaquo Fe2 center is H-bonded to six different sulfonate oxygen atoms from six different **L** and six MeOH molecules. Still, as the thermal analysis data to be discussed will show, these interactions are not as stabilizing as the encapsulating H-bonds to the hexaaquo Fe1 center. The second-sphere bonding about a single Fe1 center and its extension to the surrounding Fe2 centers is shown in Figure 9a. Down the *c*-axis, the second-sphere complexes alternate in a column with the "naked" hexaaquo Fe2 centers. Separating these two moieties is a layer of three MeOH molecules. In addition to the previously mentioned water molecule coordinated to Fe2, the methanol molecule is also involved in hydrogen bonding to one of the sulfonate oxygen atoms already forming a H-bond to the water coordinated to Fe1 (O6···O5 = 2.769(3) Å). The overall packing is

(17) Many elegant examples of supramolecular capsules exist, employing noncovalent and coordinate covalent bonding. For a general sampling, the reader is referred to the following: (a) Maverick, E.; Cram, D. J. In *Comprehensive Supramolecular Chemistry*; Atwood, J. L., Davies, J. E. D., MacNicol, D. D., Vögtle, F., Lehn, J.-M.; Elsevier Science: New York, 1996; Vol. 2, p 367. (b) Rebek, J., Jr. *Acc. Chem. Res.* **1999**, *32*, 278. (c) Atwood, J. L.; Barbour, L. J.; Hardie, M. J.; Raston, C. L. *Coord. Chem. Rev.* **2001**, *222*, 3. (d) Fujita, M. *Chem. Soc. Rev.* **1998**, *6*, 417. (e) Leininger, S.; Olenyuk, B.; Stang, P. J. *Chem. Rev.* **2000**, *100*, 853. (f) Jaset, A.; Sherman, J. C. *Chem. Rev.* **1999**, *99*, 931. (g) Sijbesma, R. P.; Meijer, E. W. *Curr. Opin. Colloid Interface Sci.* **1999**, *4*, 24. (h) Conn, M. M.; Rebek, J., Jr. *Chem. Rev.* **1997**, *97*, 1647. (i) Olenyuk, B.; Whiteford, J. A.; Fechtenkotter, A.; Stang, P. J. *Nature* **1999**, *398*, 796. (j) MacGillivray, L. R.; Atwood, J. L. *Nature* **1997**, *389*, 469. (k) Timmerman, P.; Nierop, K. G. A.; Brinks, E. A.; Verboom, W.; van Veggel, F. C. J. M.; van Hoorn, W. P.; Reinhoudt, D. N. *Chem.—Eur. J.* **1995**, *1*, 132. (l) Fochi, F.; Jacopozzi, P.; Wegelius, E.; Rissanen, K.; Cozzini, P.; Marastoni, E.; Fisiciaro, E.; Manini, P.; Fokkens, R.; Dalcanale, E. *J. Am. Chem. Soc.* **2001**, *123*, 7539. (m) Ziegler, M.; Brumaghim, J. L.; Raymond, K. N. *Angew. Chem., Int. Ed.* **2000**, *39*, 4119. (n) Hof, F.; Craig, S. L.; Nuckolls, C.; Rebek, J. *Angew. Chem., Int. Ed.* **2002**, *41*, 1488.

(18) Huheey, J. E.; Keiter, E. A.; Keiter, R. L. *Inorganic Chemistry*; Harper Collins: New York, 1993.

(19) (a) Russell, V. A.; Evans, C. C.; Li, W.; Ward, M. D. *Science* **1997**, *276*, 575. (b) Holman, K. T.; Martin, S. M.; Parker, D. P.; Ward, M. D. *J. Am. Chem. Soc.* **2001**, *123*, 4421. (c) Swift, J. A.; Pivovar, A. M.; Reynolds, A. R.; Ward, M. D. *J. Am. Chem. Soc.* **1998**, *120*, 5887. (d) Holman, K. T.; Pivovar, A. M.; Swift, J. A.; Ward, M. D. *Acc. Chem. Res.* **2001**, *34*, 107. (e) Holman, K. T.; Pivovar, A. M.; Ward, M. D. *Science* **2001**, *294*, 1907.
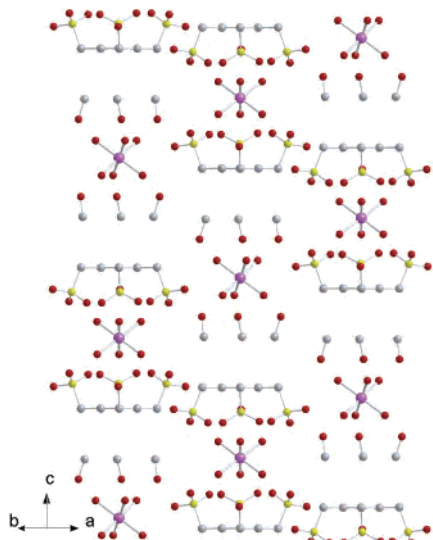
Figure 2. View of **1** perpendicular to the *c*-axis showing the offset alignment of adjacent columns and the placement of the MeOH molecules.
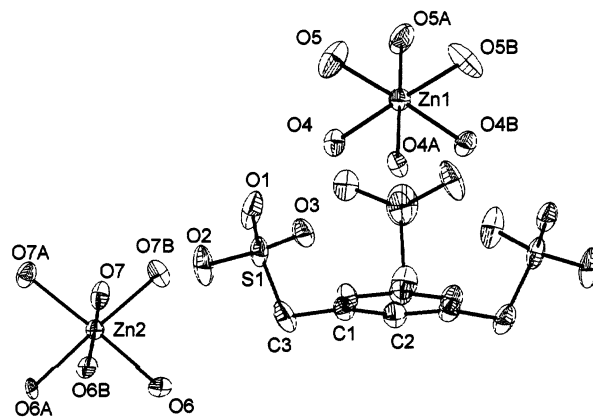

Figure 3. ORTEP plot of **4** showing the numbering scheme and the half-encapsulated hexaaquo Zn1 center as well as the intrachannel hexaaquo Zn2 center. Thermal ellipsoids of 50% probability are represented.

shown in Figure 2. Adjacent columns along the *c*-axis are offset by 7.954(2) Å, corresponding to a third the length of the *c*-axis. Thus, a fourth column added to Figure 2 would align laterally with the first. The hydrogen-bonding arrays about each of the Fe1 and Fe2 centers are shown in Figure 10a,b.

Structures of Half-Encapsulated Species: [Zn$_{1.5}$(H$_2$O)$_9$L], 4; [Mg$_{1.5}$(H$_2$O)$_9$L], 5; [Cu$_{1.5}$(H$_2$O)$_9$L]·1.3H$_2$O, 6. With divalent hexaaquo complexes as compared to the trivalent species, there is only two-thirds of the cationic charge present to attract the sulfonate ligands; as such, rather than complete capsules being formed, half-capsules are observed. In this series, compounds **4** and **5** are isostructural and based upon octahedral coordination spheres. The compounds crystallize in the chiral space group *P*6. Only the Zn complex, **4**, will be discussed in detail as, again, the Mg complex, **5**, possesses only slight variations in thermal and structural parameters to **4** as can be ascertained from the Supporting Information. Compound **6**, the Cu(II) complex, contains a Jahn−Teller distorted geometry, typical for d^9 systems, which disrupts the efficient packing and hydrogen bonding in **6** relative to the more symmetrical **4** and **5**. Zn^{2+} (0.74 Å) and Mg^{2+} (0.71 Å) are, as with Al^{3+} and Cr^{3+}, two other ions that possess similar radii and identical charge and frequently adopt isomorphous extended solid structures.[18]

The asymmetric unit in compound **4** consists of a third of a molecule of **L**, a third of one Zn center, Zn1, with two unique water molecules bound (Zn1−O4 = 2.095(5) Å, Zn1−O5 = 2.062(6)), and a sixth of another Zn ion, Zn2, also with two types of coordinated water molecules (Zn2−O6 = 2.074(8) Å, Zn2−O7 = 2.079(8) Å), each one on a symmetry site. The hexaaquo divalent complex centered on Zn1 can be described as a "half-encapsulated" structure as **L** caps only one of the triangular triaquo faces, as compared to the double capping observed in **1**−**3**. The half-encapsulated structure is shown in the ORTEP diagram of **4** (Figure 3). As in **1**−**3**, each coordinated water molecule of the encapsulated face in **4** forms hydrogen bonds to two oxygen

atoms from two different sulfonate groups (O4···O1 = 2.697(7) Å, O4···O3 = 2.747(6) Å) and is staggered with respect to the 1,3,5-substitution pattern of the aromatic ring (Figure 9b). As would be expected, the hydrogen bonds to the divalent center are slightly longer (0.05−0.1 Å) than those observed in the trivalent complexes, **1**−**3**. From the perspective of a single sulfonate moiety, two sulfonate oxygen atoms again bridge two cis aquo ligands. The hydrogen bonding of the Zn1 center is shown in Figure 10c. Where compounds **4** and **5** differ dramatically from **1**−**3** is in the second-sphere behavior of the nonencapsulated triaquo face of the complexes. Each of these three equivalent aquo ligands form two hydrogen bonds to two sulfonate oxygen atoms from two different SO$_3$ groups (O5···O2 = 2.764(7) Å, O5···O3 = 2.856(7) Å). While, as shown in Figure 10c, the overall hydrogen bonding pattern of each face of Zn1 to the sulfonate groups is the same, for the nonencapsulated face, each sulfonate group is associated with a different molecule of **L**. Again, even though in this case the sulfonate groups originate from different ligands, the observed motif is that cis aquo ligands are bridged by a single sulfonate group. Notably, these H-bonding distances are all longer than those of the encapsulated face where the three sulfonate groups stem from the same molecule of **L**. This illustrates the significance of the chelate effect for second-sphere coordination.

For the nonencapsulated face of Zn1 of compound **4**, the SO$_3$ groups originate from three neighboring molecules of **L**, each crystallographically equivalent to the first, which are arranged in a trigonal array about the half-encapsulated complex. These ligands are displaced along *z* by half a unit cell which puts them in an ideal position to H-bond with their neighbors. The equivalence of these ligands implies they are also involved in forming half-encapsulated complexes with a symmetry-related hexaaquo complex centered on Zn1. This arrangement necessitates that all the half-encapsulated complexes align in columns and that all the complexes are oriented in the same direction as shown in Figure 4a. Interestingly, when the structure is viewed down the axis of the hydrogen-bonded columns, the *c*-axis, one sees the hexagonal channel structure formed by the interconnected half-encapsulated species. Residing in the channels is the
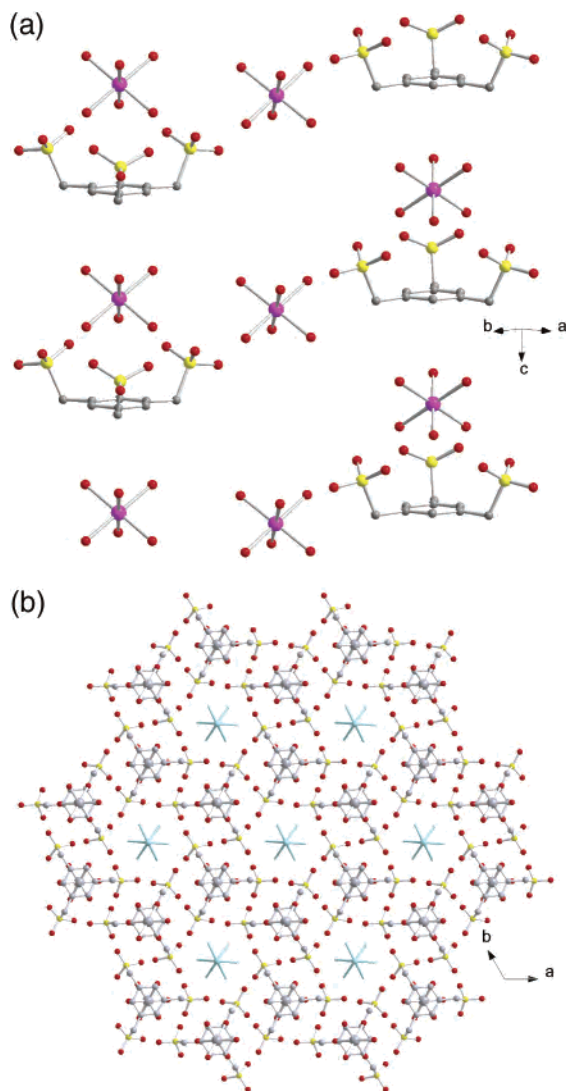
Figure 4. Views of **4**: (a) perpendicular to the *c*-axis showing the alignment of half-capsules centered on Zn1 and the relative positioning of the "naked" hexaaquo Zn2 center, where, for clarity, only one position for the Zn2 complex is shown; (b) looking down the *c*-axis showing the hexagonal H-bonded net with intrachannel $[Zn(H_2O)_6]^{2+}$.

nonencapsulated hexaaquo Zn complex centered on Zn2 as shown in Figure 4b. The $[Zn(H_2O)_6]^{2+}$ complexes are aligned with their triangular triaquo faces perpendicular to the axis of the channel. Extensive hydrogen bonding occurs between these complexes and the sulfonate groups lining the channel as shown in Figure 10d. Each aquo ligand on Zn2 forms two hydrogen bonds to two sulfonate oxygen atoms (O6···O1 = 2.727(8) Å, O6···O2 = 2.98(1), O7···O1 = 3.11(1) Å, O7···O2 = 2.59(1) Å) for a total of 12 hydrogen bonds to 6 different sulfonate groups. These centers are disordered along the *c*-axis with each position being half-occupied. The most reasonable model of this disorder would have the hexaaquo Zn2 centers repeat at a distance of 9.662(3) Å, much like the Cu analogue, **6**, which is not disordered.[20] The optimum packing of the networks for compounds **4** and **5** results in each sulfonate group acting as an acceptor for six hydrogen bonds, two from the aquo ligand on the half-encapsulated Zn1 complex, two from an aquo ligand on an adjacent Zn1 complex to form the extended structure, and
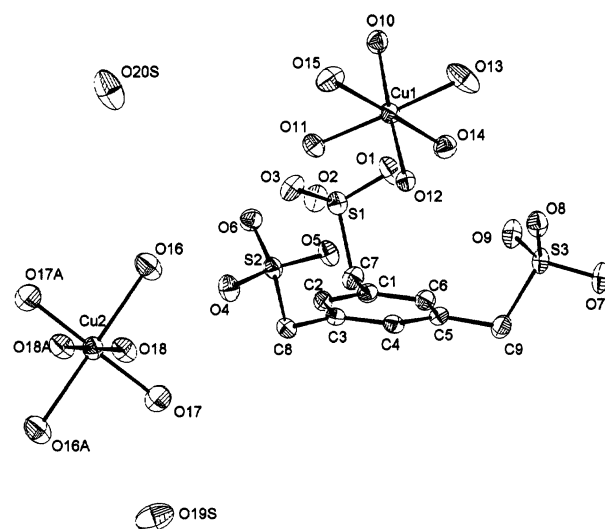
Figure 5. ORTEP plot of **6** showing the numbering scheme and the Jahn–Teller-distorted but still half-encapsulated hexaaquo Cu1 center. Also shown is the intrachannel hexaaquo Cu2 center. Thermal ellipsoids of 50% probability are represented.

two from water molecules on the hexaaquo Zn2 complexes in the channels.

Complex **6**, $[Cu_{1.5}(H_2O)_9\mathbf{L}]\cdot 1.3H_2O$, is related to complexes **4** and **5** in that it is also a hexaaquo species centered on a divalent metal. The asymmetric unit for **6** consists of a complete molecule of **L**, one full Cu center and one-half of another Cu center, nine coordinated water molecules, and water of solvation not observed in any of the previous complexes. The overall structure is similar to those of **4** and **5** but with much lower symmetry (monoclinic versus hexagonal), stemming from the fact that whereas the cationic hexaaquo species in **4** and **5**, as well as **1**– **3**, have near perfect octahedral symmetry, the Cu^{2+} centers are elongated along one axis, i.e., Jahn–Teller distortion ($Cu1-O_{eq}$ = 1.963(3)–2.013(3) Å, $Cu1-O_{ax}$ = 2.227(3), 2.230(3) Å, $Cu2-O_{eq}$ = 1.962(3)–1.991(3) Å, $Cu2-O_{ax}$ = 2.324(3) Å). The net result of this elongation is that there is a reduction in the complementarity of the now distorted triangular faces of the metal centers with the trisulfonated ligand. As with **4** and **5**, a half-encapsulated complex is formed between **L** and one of the triangular faces of a hexaaquo complex, in this case centered on Cu1, but all hydrogen-bonding interactions are inequivalent, ranging from 2.704(4) to 2.789(4) Å. Figure 5 shows an ORTEP representation of **6**. The external faces of the sulfonate groups are involved in a total of 12 different hydrogen bonds to water molecules associated with the six surrounding hexaaquo Cu centers ($O_{donor}-O_{acc}$ = 2.708(4)–2.954(4) Å), shown in Figure 9c, to form quasi-hexagonal channels, shown in Figure 6b. For Cu1, the Jahn–Teller distortion does not prohibit the bridging of *cis*-aquo ligands by a single sulfonate group even where the elongated

(20) The alternating orientation of hexaaquo complexes centered on Zn2 is corroborated by examining the thermal parameters for the sulfonate oxygen atoms that hydrogen bond along the periphery of the channel. Essentially, throughout the crystal, these oxygen atoms occupy two different positions, one directed toward each alternatingly present hexaaquo ion. The two different positions are not resolved but instead are manifested as the large thermal parameters observed for atoms O1 and O2 as they are centered on an intermediate position.
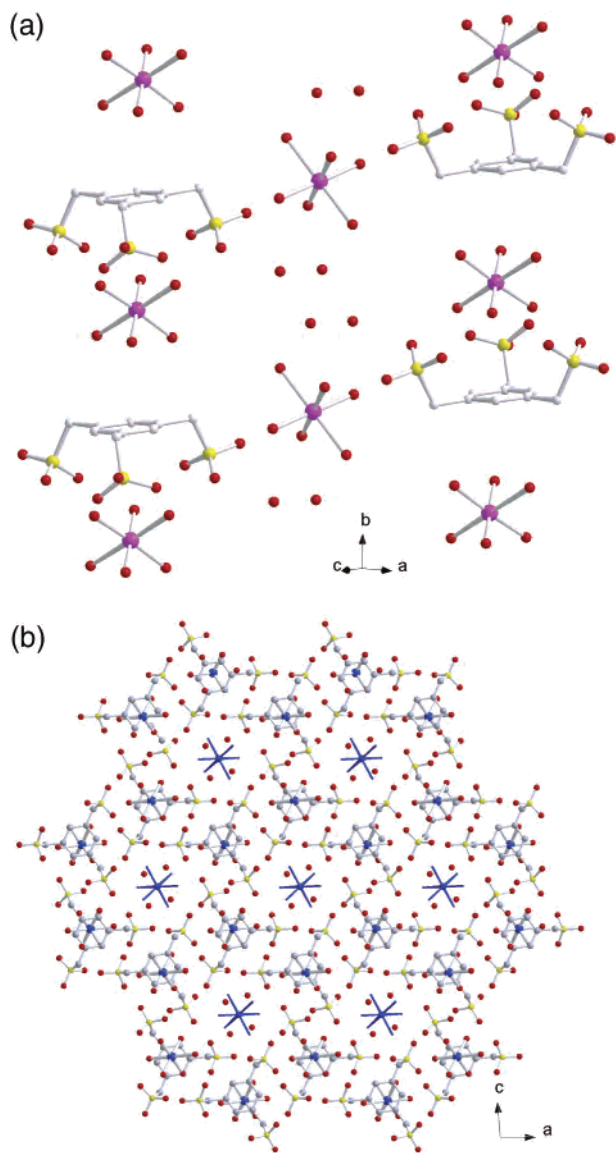
Figure 6. Views of **6**: (a) perpendicular to the *c*-axis showing the alignment of half-capsules centered on Cu1 and the relative positioning of the "naked" hexaaquo Cu2 center; (b) looking down the *c*-axis showing the quasi-hexagonal H-bonded net with intrachannel $[Cu(H_2O)_6]^{2+}$ and water molecules.

Figure 7. ORTEP plot of **7** showing the numbering scheme and the cis−trans−trans conformation of **L**. Thermal ellipsoids of 50% probability are represented.

Figure 8. Views of **7** perpendicular to the *c*-axis showing the layers of $[Co(NH_3)_6]^{3+}$ bridged by hydrogen-bonded molecules of **L**.

sites are involved. In contrast to **4** and **5**, where all the columns of half-encapsulated metal centers are identical and have the same orientation, for **6**, three of the six columns surrounding the hexagonal channels have their half-capsules pointing in the opposite direction (Figure 6a). The columns with opposite orientation are all diametrically opposed with three adjacent columns pointing in the same direction. If one looks at the overall packing of the hexagons, each column borders, and forms hydrogen bonds with, two adjacent columns oriented in the same direction and one pointing in the opposite direction. Once again, within the channels resides the second crystallographic hexaaquo metal complex, centered on Cu2 (Figure 6b). In this case, there are also two molecules of uncoordinated water present. As with **4** and **5**, the hexaaquo complexes in the channel are extensively H-bonded to SO₃ groups. In **6**, this is diminished at the cost of additional hydrogen bonding to the free water molecules
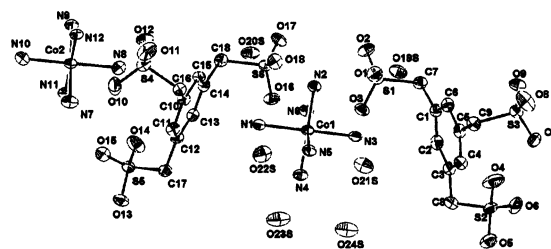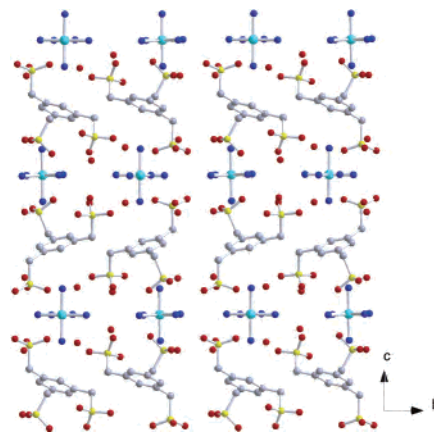
in the channels. For the hexaaquo complex centered on Cu2, only four sulfonate groups, of a possible six, form the prevalent "*cis*-aquo" bridging motif. Surprisingly, the two sulfonate groups which do not form this motif are sulfonate bridges between equatorial cis sites. The sulfonate bridges between equatorial sites and the axially elongated sites remain intact. The total hydrogen-bonding arrays about the Cu1 and Cu2 centers are shown in Figure 10e,f, respectively. Adjacent $[Cu(H_2O)_6]^{2+}$ units in the channels are separated by 9.418(3) Å, which is a slightly shorter value than that observed in **4** and **5**.

From the perspective of crystal engineering, it is interesting to note the macroscopic structural changes which are brought about by employing a Jahn−Teller-distorted divalent hexaaquo metal in **6**, in place of the octahedral divalent hexaaquo metals in **4** and **5**. Clearly, there is a loss of complementarity between the triaquo faces of the axially elongated complex and **L** relative to the more perfectly triangular faces in an octahedron. The second-sphere interactions of the non-encapsulated triaquo face of the Cu centers are also desymmetrized. This in turns disrupts the delicate intermolecular hydrogen-bonding network responsible for the perfect hexagonal columns observed in **4** and **5** and results in inclusion of guest water molecules as well as the reversal of the orientation of half the column structures.

Structure of the Extended Complex, $[Co(NH_3)_6]_2(L)_2 \cdot 6H_2O$, 7. The structure of **7**, from a macroscopic perspective, can be described as a two-dimensional array of hexaammine Co centers linked in the layers via hydrogen bonding to sulfonate groups and "pillared" in the third dimension by the mesitylene unit of **L** (Figures 7 and 8). From a molecular
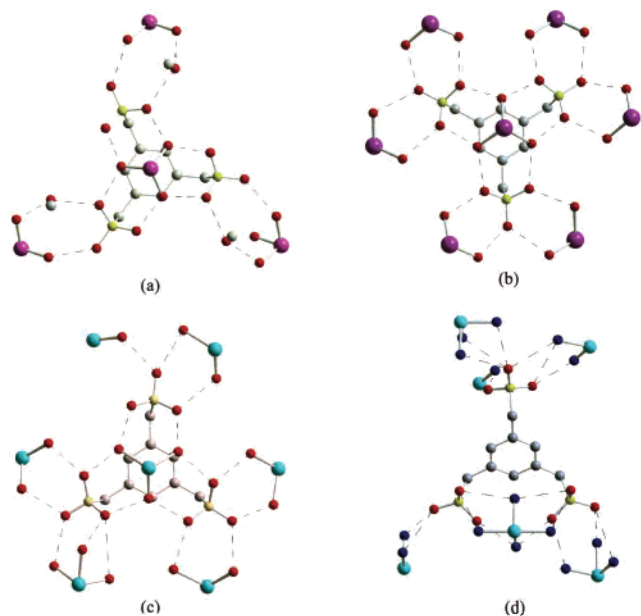
Figure 9. Comparison of the hydrogen-bonding patterns observed to the sulfonate groups of **L** from the following metal complexes: (a) the trivalent hexaaquo complexes, **1**–**3**; (b) the divalent hexaaquo complexes, **4** and **5**; (c) the Jahn–Teller-distorted, divalent hexaaquo complex, **6**; (d) the trivalent hexaammine complex, **7**. Only one molecule of **L** is shown for **7**.

viewpoint, these structural changes can again be traced to the complementary of hydrogen bonding between the coordinated ligands and **L**. The asymmetric unit for **7** is comprised of two distinct $[Co(NH_3)_6]^{3+}$ centers, two molecules of **L**, and six molecules of water. Both Co centers have a near perfect octahedral geometry (Co1–N = 1.954(5)–1.981(6) Å, Co2–N = 1.956(6)–1.981(6) Å) and are oriented with their equatorial planes parallel to the layers in the *ab* plane. The perpendicular distance between layers is 10.45(1)–10.49(1) Å depending on the atoms chosen. Both Co1 and Co2 centers occur in each layer. Within a layer, like metal centers align along the *a*-axis at a distance of 7.903(2) Å and alternate along the *b*-axis at a distance of 7.331(2) Å. The hydrogen-bonding environments about each ligand and metal center are actually quite similar. Both types of ligand occur in a cis–trans–trans conformation and hydrogen bond to 6 different hexaammine complexes via a total of 12 different hydrogen bonds, as shown in Figure 9d. The two sulfonate groups oriented on the same side of the aromatic ring in **L** are situated along two of the edges of a triangle of $Co(NH_3)_6$ complexes whereas the sole sulfonate group pointing to the opposite side is situated in the middle of a triangle of three other metal centers. Hydrogen bonds to the sulfonate oxygen atoms of the first type of ligand from the NH_3 groups range from 2.948(8) to 3.280(8) Å with respect to donor–acceptor separation. This range spans 2.886(8)– 3.316(8) Å for the second molecule of **L**. Conversely, the hexaammine complex centered on Co1 has numerous oxygen atoms within hydrogen-bonding contact distance. In this case, there are a total of 15 oxygen atoms, from 5 water molecules and 10 sulfonate oxygen atoms, as shown in Figure 10g. The 10 sulfonate oxygen atoms originate from six different sulfonate groups each from a different molecule of **L**. Each hexaammine cobalt complex
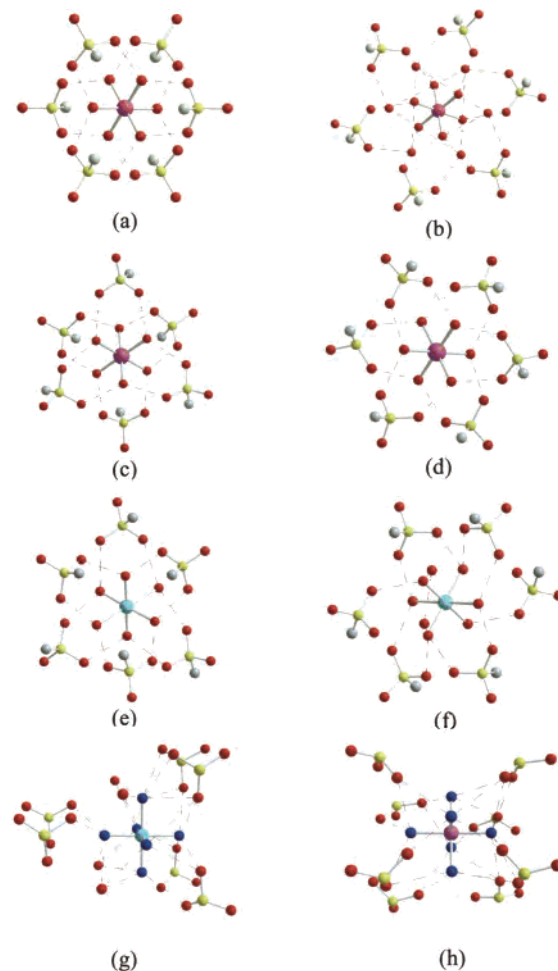
Figure 10. Hydrogen-bonding patterns between sulfonate oxygen atoms and water molecules for the metal centers in compounds **1**–**7**: (a) **1**, the fully encapsulated hexaaquo complex centered on Fe1; (b) **1**, the "naked" hexaaquo center on Fe2; (c) **4**, the half-encapsulated hexaaquo complex centered on Zn1; (d) **4**, the "naked" hexaaquo complex in the channels centered on Zn2; (e) **6**, the half-encapsulated, Jahn–Teller-distorted, hexaaquo complex centered on Cu1; (f) **6**, the "naked", Jahn–Teller-distorted, hexaaquo complex in the channels centered on Cu2; (g) **7**, the hexaammine complex which interacts with the free water molecules centered on Co1; (h) **7**, the hexaammine complex which does not interact with water molecules, centered on Co2.

centered on Co2 forms hydrogen bonds to eight different sulfonate groups from six different molecules of **L**, as shown in Figure 10h. In total, there are 13 oxygen atoms which are situated at a reasonable distance and orientation to be acting as hydrogen bond acceptors from the NH_3 groups on Co2. Undoubtedly, for both Co centers, some of these interactions involve bifurcated H-bonds but exact assignments are not discernible without locating the hydrogen positions empirically.

Hydrogen-Bonding Motifs. As illustrated by Figures 9 and 10, in the aquo complexes of both trivalent and divalent metal ions, the predominant hydrogen-bonding motif is the association of *cis*-aquo ligands on the metal center and two oxygen atoms from the same sulfonate group. In the absence of other structural constraints, this motif is unquestionably prevailing.[12] For example, in the complex, $[Fe(H_2O)_6](CF_3-SO_3)_2$, the *cis*-aquo sulfonate motif is maximized as six different sulfonate groups each form two hydrogen bonds

to the Fe complex.[12a] Despite ligand constraints, this motif is also maximized in the divalent octahedral complexes **4** and **5** (Figures 9b and 10c,d).

In the hexaammine structures, the hydrogen bonding pattern of *cis*-NH₃ ligands with the sulfonate oxygen atoms is completely altered. In **7**, the mode of interaction of the sulfonate groups with the hexaammine Co centers is highly variable. The principal difference is that, in **7**, a single oxygen atom from a sulfonate group frequently acts to bridge either two *cis*-NH₃ groups or even to cap three mutually *cis*-NH₃ groups. This is observed for only one individual sulfonate oxygen atom in all the aquo complexes **1−6** and occurs in the Jahn−Teller-distorted complex, **6**. Of the 10 sulfonate oxygen atoms which hydrogen bond to the hexaammine Co1 center, four adopt cis bridging or capping modes while the other six interact with only one NH₃ group. The Co1 center is not ideal to ascertain the sulfonate interactions with the hexaammine complex as the hydrogen bonding is disrupted by the crystallized water molecules. The hexaammine Co2 complex does not interact with the water of solvation. In this case, of the 13 sulfonate oxygen atoms which hydrogen bond to a single hexaammine complex, *10* adopt the single sulfonate oxygen bridging mode observed only once in the aquo complexes and that in the Jahn−Teller distorted **6**.

Thermal Analysis. Thermogravimetric analyses (TGA) were performed on complexes **1−6**, and similar trends were observed in the mass losses for related compounds. Specifically for **1−3**, the following trends were observed: Loss of the guest MeOH molecules was rapid, beginning at room temperature to ∼110 °C (15.6% calcd, 15.9% obsd). This merges with a second mass loss of six water molecules (8.75% calcd, 8.95% obsd) up to ∼160 °C. Continuing, to ∼265 °C, six water molecules (8.75% calcd, 8.99% obsd) are lost to fully desolvate the complex. The final mass loss, above 300 °C, corresponds to decomposition of **L**. Typically, aquo ions in transition metal complexes are lost at temperatures below 150 °C.[21] This correlates very well with the first loss of water observed in **1**, to be assigned to the "naked" metal cation. The temperature of the second mass loss then shows that the aquo ligands of the encapsulated metal center have been stabilized by >100 °C through the secondary coordination sphere, a very significant value given that only weak interactions are involved. Undoubtedly, the disruption of H₂O−sulfonate hydrogen bonding by the incorporation of the more volatile methanol molecules (Figure 10b) plays a significant role in facilitating the loss of the aquo ligands on the "naked" metal center. The TGA data for **1−3** are shown in Figure 11 for comparison.

For complexes **4−6**, the TGA data are again similar (Figure 12), as they are all networks containing half-encapsulated hexaaquo ions. The TGA data for complexes **4** and **5** show a rapid loss of mass beginning at ∼50 °C and continuing to ∼150 °C with an additional small mass loss
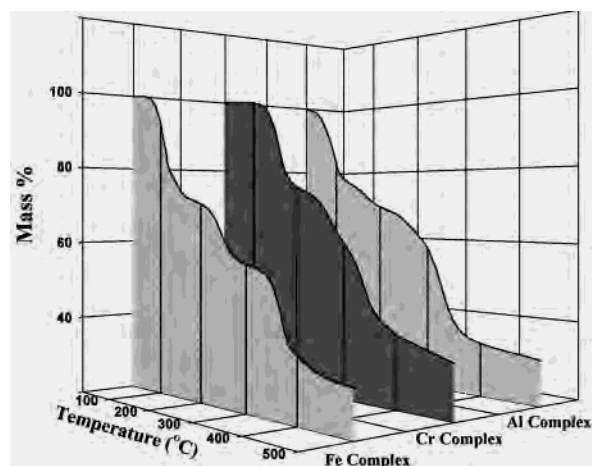

Figure 11. TGA data for the fully encapsulated complexes, **1−3**, of trivalent hexaaquo ions.
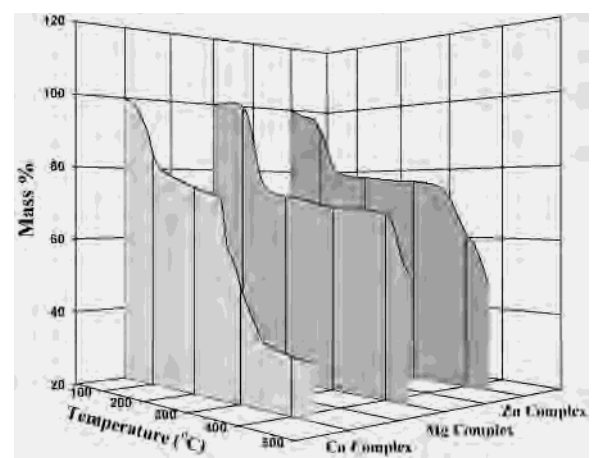

Figure 12. TGA data for the half-encapsulated complexes, **4−6**, of divalent hexaaquo ions.

continuing up to just prior to the ligand decomposition. These mass losses corresponds very well to the removal of all the aquo ligands in the complex (26.4% calcd and 24.0% obsd for **4**, 29.2% calcd and 29.0% obsd for **5**). In **4** and **5**, all aquo ligands form two hydrogen bonds to two different sulfonate groups, as shown in Figure 10c,d. The observation that the aquo ligands of the single encapsulated face in these complexes are not as markedly stabilized as in **1−3** is attributed not so much to the lack of complete encapsulation of the hexaaquo ion but more to the dicationic, versus tricationic, charge on the metal center. Indeed, the donor−acceptor distances in the encapsulating hydrogen bonds in **1−3** (2.629−2.644 Å) are all significantly shorter than their counterparts in **4** and **5** (2.715−2.758 Å). Compound **6** is similar to **4** and **5** but, owing to the Jahn−Teller-distorted Cu centers, incorporates 1.3 molecules of guest water/unit. The TGA data for this compound correspond well to the complete loss of both coordinated and guest water molecules up to 240 °C (29.1% calcd, 28.3% obsd).

Conclusions

The second-sphere coordination chemistry of a novel trisulfonated ligand has been presented. With trivalent hexaaquo ions, intramolecular second-sphere capsules are

(21) (a) Apblett, A. W.; Cubano, L. A.; Georgieva, G. D.; Mague, J. T. *Chem. Mater.* **1996**, *8*, 650. (b) Maleki, A.; Gajerski, R.; Labus, S.; Prochowska-Klisch, B.; Wojciechowski, K. T. *J. Therm. Anal. Calorim.* **2000**, *60*, 17. (c) Langfelderova, H. *J. Therm. Anal.* **1994**, *41*, 955. (d) Kanungo, S. B.; Mishra, S. K. *J. Therm. Anal.* **1997**, *48*, 385. (e) Maneva, M.; Kovandjiev, P. *J. Therm. Anal.* **1993**, *39*, 1347.

formed where the primary aquo sphere is stabilized by over 100 °C owing to both the 3+ charge on the metal and the high complementarity of the ligand with the triangular aquo faces of the complex. With divalent hexaaquo ions, only half-capsules are formed which self-associate intermolecularly to form extended hydrogen-bonded nets. The dominant hydrogen-bonding pattern observed in both these systems is the complementarity between adjacent oxygen atoms of a sulfonate group and *cis*-oriented aquo ligands on the metal center. Given the recurrent nature of this interaction in aquated metal complexes with sulfonate anions, it has promise as a new supramolecular synthon. If the divalent ion is a Jahn−Teller-distorted Cu(II) center, the complementarity is reduced, packing efficiency is decreased, and guest inclusion is observed. Inversion of the orientation of half the columns of compounds in the structure was also observed. For a trivalent hexaamminemetal ion, the dominant hydrogen-bonding motif becomes the bridging of mutually *cis*-NH$_3$ sites by a single sulfonate oxygen atom, involving either two or three amine sites. In the amine structure, no encapsulation of any kind is observed and an extended framework was formed. These results serve to illustrate many of the core principles of supramolecular chemistry, those being the importance of preorganization, complementarity, and cooperativity between intermolecular interactions. We have shown how altering the complementarity between primary and secondary sphere ligands effects both the structure and physical properties of supramolecular second-sphere complexes. In a more general sense, these results have implications for the assembly and stabilization of discrete metal complexes in the solid state.

Supporting Information Available: X-ray crystallographic files for compounds **1**−**7**, in CIF format. This material is available free of charge via the Internet at http://pubs.acs.org.

IC025627S